

## ORBIT DETERMINATION RESULTS FOR THE CASSINI TITAN-A FLYBY

**Ian M. Roundhill, Peter G. Antreasian, Kevin E. Criddle, Rodica Ionasescu,  
M. Cameron Meek, and Jason R. Stauch\***

This paper describes Cassini orbit determination results from the first targeted flyby of Titan. The orbit determination model is outlined including the radiometric and optical data and the parameter estimation for the Cassini, Saturn, and satellite trajectories. The solutions computed to support maneuver decision points are described along with alternate solution used to gain confidence in the baseline strategy. Finally, the reconstructed flyby conditions are compared to the prediction to reveal a Titan ephemeris error. The optical data model is then examined to reveal why this error was not observable.

### INTRODUCTION

The Cassini-Huygens mission was launched on October 15, 1997 as a joint NASA/ESA mission to explore Saturn. After a 7 year cruise the spacecraft entered orbit around Saturn on July 1, 2004 for a 4 year investigation of the Saturnian system. One key element of the Cassini mission is the exploration of Titan with 45 targeted flybys of this satellite. This paper describes the orbit determination analysis and results for the first targeted flyby of Titan, the Titan-A flyby, on October 26, 2004.

In the following sections information will be provided about the orbit determination model, the solution history, and the observability of Titan's ephemeris. The orbit determination model includes information about the radiometric and optical data collected for navigation purposes and the parameter estimation assumptions. Parameters for Cassini, Saturn, the Saturnian satellites, and the measurements are described.

The solution history for three maneuver decision points is then described. Alternate solutions with different assumptions were used to identify areas of mismodeling. Some of the assumptions being tested were choice of epoch, non-gravitational constraints, optical weights, data sets, and satellite state constraints.

Finally, the reconstructed flyby results are compared to the predicted results. This comparison reveals a shift in the Titan ephemeris that was not detected prior to the flyby. The optical data model and observability of the Titan ephemeris is examined.

---

\* Outer Planet Flight Dynamics, Jet Propulsion Laboratory, California Institute of Technology, 4800 Oak Grove Drive, California 91109.

# ORBIT DETERMINATION MODEL

## Epoch Choice

Four different initial times were used for the Titan A Orbit Determination; June 21<sup>st</sup>, July 1<sup>st</sup>, July 17<sup>th</sup>, and October 5<sup>th</sup>. The June date was chosen to be before Saturn periapse and after the final approach optical navigation picture. The second date was immediately after a large spacecraft maneuver for Saturn Orbit Insertion (SOI). The third date was near the end of solar conjunction. The fourth date was after a week of thruster firings due to Reaction Control System (RCS) control; there was no thruster activity after this date.

## Radiometric Data

Two-way coherent X-band Doppler and range data was collected using the Deep Space Network (DSN) for approximately 6 hours every day. Only stations in Southern California and Spain were used because of poor geometry from Australian stations. Both the 2-way and 3-way Doppler were weighted on a per-pass basis to the standard deviation multiplied by a scale factor of 3.36 and the residuals are shown in Figures 2 and 3. The ranging data was collected concurrently with the 2-way Doppler data and was weighted with the same algorithm and residuals are shown in Figures 4 and 5. This time span also includes the effects of solar conjunction when the Sun passed near the spacecraft-Earth line and the radiometric data from the beginning of the arc until July 25, 2004 was deweighted by a factor of two.

## Optical Navigation Data

Optical navigation (opnav) data is used by Cassini to refine the orbits of the target satellites. The Narrow Angle Camera onboard Cassini is used to take pictures of Saturnian satellites while known stars are in the background. The optical navigation team measures the two-dimensional location of the satellites and stars in the image. These measurements along with the known locations of the stars are provided to the orbit determination team. The star measurements are primarily used to orient the image and the satellite measurements are used to refine the satellite and/or spacecraft trajectory.

Optical navigation data was collected from July 2, 2004 to October 27, 2004. Due to solar conjunction, no images were taken from July 3<sup>rd</sup> to July 12<sup>th</sup>. The distribution of satellites imaged is shown below:

**Table 1: Distribution of Opnavs by Satellite**

Satellite	Number	Satellite	Number
Mimas	52	Rhea	46
Enceladus	42	Titan	57
Tethys	42	Hyperion	44
Dione	51	Iapetus	41

The sigmas applied to each measurement varied by satellite and by range yielding values from 0.25 to 1.0 pixels except for Titan and Iapetus, which peaked at 5 pixels. Many of the satellites had interesting features (atmosphere, craters, chaotic pole direction, bulges and ridges) and the optical navigation team compensated by computing weights that increased the measurement uncertainty as the range decreased.

## Parameter Estimation

Various parameters were estimated to adjust the spacecraft model, the planetary and satellite model, and the measurement model. These parameters may be estimated as a bias value constant over the entire arc or a stochastic set of values that change over time. If not estimated, a parameter may be “considered” to allow for uncertainties in the variable to be included in the estimation process.

*Spacecraft Models.* The spacecraft models include several sub-elements. The initial state was estimated as position and velocity in a Cartesian frame with an infinite a priori uncertainty. The state may also be constrained by a postfit uncertainties from the previous data fit. The thermal force due to the radioisotope thermoelectric generators (RTG) radiation was modeled as an exponential decay model with an estimated scale parameter in each of the spacecraft axes. The spacecraft axes were oriented using a predicted attitude profile provided by the spacecraft team. The force due to solar pressure was included with nominal reflectivity values but no parameters were estimated. Three Orbit Trim Maneuvers (OTM) were executed using the spacecraft main engine and the estimated parameters were  $\Delta V$ , right ascension, declination and start time.

Thrusting due to the RCS included a widely varying set of models. Some events were very short in duration and directed along the spacecraft-Earth line during radiometric tracking. Other events were longer in duration and/or included components perpendicular to the radiometric measurements.

**Table 2: Thrusting Events Due to Reaction Control System**

Date	Event	$\Delta V$ on Earthline	Model
Jul 3	Wheel bias	Yes	One small force
Jul 11	Wheel bias	Yes	One small force
Jul 14	Probe Checkout 14	Yes	One impulse, an estimated acceleration along Earthline during 10 hours of RCS control, and another impulse.
Jul 17	Wheel bias	Yes	One small force
Jul 30	Wheel bias	Yes	One small force
Aug 13	Wheel bias	Yes	One small force
Aug 23	OTM002		One small force before and after OTM.
Aug 30	Friction Test	Yes	Three small forces
Sep 7	OTM003		One small force before and after OTM
Sep 12	Wheel Bias & Friction Test	Yes	Thruster control during varying wheel speeds. Modeled with 4 small forces and a stochastic spacecraft Z-axis acceleration.
Sep 14	Probe Checkout 15	Yes	One impulse, an estimated acceleration along Earthline during 10 hours of RCS control, and another impulse.
Sep 23	Wheel Bias	Yes	One impulsive event
Oct 2-5	Load AACS Software		Spacecraft fixed stochastic accelerations over entire time period.
Oct 2	Transition to thrusters	Yes	One small force
Oct 3	Deadband changes	Yes	Two small forces
Oct 4	Detumble test	No	One impulsive maneuver in each of X, Y, and Z with different duration estimate for each.
Oct 5	Transition to RWA	Yes	One small force
Oct 23	OTM004	No	One small force immediately after maneuver because of deadband reduction and another small force a few hours after maneuver.
Oct 26	Ta events	No	AACS FSDS thruster predictions modeled with miscellaneous force model. Spacecraft fixed stochastic accelerations over flyby period.

Finally, to account for any force mismodeling a set of stochastic parameters were estimated in spacecraft fixed axes. These forces were estimated at  $1.25 \times 10^{-12}$  km/s<sup>2</sup> with batches every 8 hours with no correlation between batches.

*Planetary and Satellite Models.* The satellite model includes the estimation of the initial position and velocity of Mimas, Enceladus, Tethys, Dione, Rhea, Titan, Hyperion, and Iapetus at January 2, 2004. The mass of Hyperion was considered and the remaining satellite masses were estimated. The trajectory of Saturn was estimated via the Set III parameters and the Saturn Barycenter mass, J2, J4, J6, and the Saturn pole orientation were also estimated. The apriori covariance for the planet and satellite was provided from a solution with Earth-based and preceding Cassini data. This covariance would be updated with the additional of new Earth-based data or refinement of the preceding Cassini data.

*Measurement Models.* The radiometric measurement models include many estimated and considered parameters. The station locations (2-3 cm), troposphere (1 cm), ionosphere (15 cm day and 4 cm night), and earth orientation (2 cm) were all considered. A per-station and per-pass ranging bias was estimated at 1 meter and 3 meters. Radiometric data near solar conjunction was adjusted by the use of solar corona parameters estimated as bias and stochastic parameters at 1 hour intervals with a 3 hour time constant. The apriori values for the solar corona A and B parameters were 8,000 and 36,000 meters.

The optical measurements were adjusted by estimating pointing corrections per picture with an apriori sigma of 1 degree per axis. The Titan pictures also included an estimate of the 0<sup>th</sup> order phase bias with an apriori sigma of 5%. The phase bias is corrected in the image along the sun-line direction and was used to account for mismodeling of the atmosphere.

**Table 3: Filter Parameters**

Name		Comments
<b>Data</b>	<b>Weight</b>	
Coherent Doppler data	Weight by pass scaled by 3.36	
Ranging data		
Opnavs	0.25 to 5 pixels	
Stars	Maximum of formal sigma and 0.1 pixels	
<b>Estimated Parameters</b>	<b>Modeled A Priori 1<math>\sigma</math> Error (Estimated)</b>	
Spacecraft epoch state	infinite	
Maneuvers		
OTM002/PRM		
$\Delta V$	785.9 mm/s	
RA	0.2 degrees	
Dec	0.2 degrees	
Start time	10 seconds	
OTM003/PRMCU		
$\Delta V$	10.0 mm/s	
RA	7.2 degrees	
Dec	2.0 degrees	
Start time	10 seconds	
OTM004/Ta-3		
$\Delta V$	8.3 mm/s	
RA	1.0 degrees	
Dec	0.9 degrees	
Thrust	0.14 N	
Stochastic non-gravitational acceleration	$1.25 \times 10^{-12}$ km/s <sup>2</sup>	
RTG acceleration bias terms	$6.25 \times 10^{-13}$ , $5.837 \times 10^{-13}$ , $6.687 \times 10^{-14}$ km/s <sup>2</sup> in spacecraft Z,X,Y.	
RCS Events	5 mm/s (typical)	See Table 2
Mimas Position and Velocity	7.41 km and 516 mm/s	
Enceladus Position and Velocity	5.26 km and 302 mm/s	
Tethys Position and Velocity	7.37 km and 264 mm/s	
Dione Position and Velocity	10.81 km and 216 mm/s	
Rhea Position and Velocity	7.96 km and 113 mm/s	
Titan Position and Velocity	11.78 km and 51.3 mm/s	
Hyperion Position and Velocity	27.07 km and 106 mm/s	
Iapetus Position and Velocity	13.07 km and 12.3 mm/s	
Saturn Position and Velocity	46.85 km and 1.19 mm/s	

**Table 3: Filter Parameters (continued)**

Mimas GM	0.0060 km <sup>3</sup> /s <sup>2</sup>	
Enceladus GM	0.28 km <sup>3</sup> /s <sup>2</sup>	
Tethys GM	0.0036 km <sup>3</sup> /s <sup>2</sup>	
Dione GM	0.0019 km <sup>3</sup> /s <sup>2</sup>	
Rhea GM	1.6 km <sup>3</sup> /s <sup>2</sup>	
Titan GM	0.98 km <sup>3</sup> /s <sup>2</sup>	
Iapetus GM	4.5 km <sup>3</sup> /s <sup>2</sup>	
Saturn Barycenter GM	17.7 km <sup>3</sup> /s <sup>2</sup>	
Saturn J2, J4, J6	1.8 e-6 8.1 e-6 8.3 e-6	
Saturn Pole Right Ascension and Declination	3.6 × 10 <sup>-3</sup> degrees 1.8 × 10 <sup>-4</sup> degrees	
Range biases per station	1 meter	
Range biases per pass	3 meters	
Stochastic camera pointing	1 degree each in 3-axes	
Titan Phase Bias	5%	
<b>Consider Parameters</b>	<b>Unmodeled A Priori 1σ Error (Considered)</b>	
Station locations	2-3 cm	
Troposphere	1.0 cm	
Ionosphere	15 cm day 4 cm night	
Earth orientation parameters	2 cm per axis	
Hyperion GM	0.1 km <sup>3</sup> /s <sup>2</sup>	

## SOLUTION HISTORY

### OTM-002 Delivery

The first maneuver to target to the Titan-A flyby was scheduled for Aug 23, 2004. This maneuver was near apoapse and designed to raise the periapse of the orbit. The target conditions for the flyby was a 1200 km altitude at Oct 26, 2004 15:30:09 ET. This target came out of the latest reference trajectory, which was used for the design of the scientific observations.

Orbit determination solutions were computed from June 26<sup>th</sup> until August 17<sup>th</sup> to support the design of OTM-002. Various deliveries were made prior to the final design and are shown with the final solution below in Figure 1. One immediately notices that one ellipse is separated from the others. The ellipses on the right were computed using the June 21<sup>st</sup> epoch but the ellipse on the left used the July 17<sup>th</sup> epoch. All of these solutions include a fixed OTM-002 design that was computed soon after SOI. Without a nominal design for OTM-002 the Titan-A flyby conditions are difficult to compute because a very different flyby is performed without the maneuver.

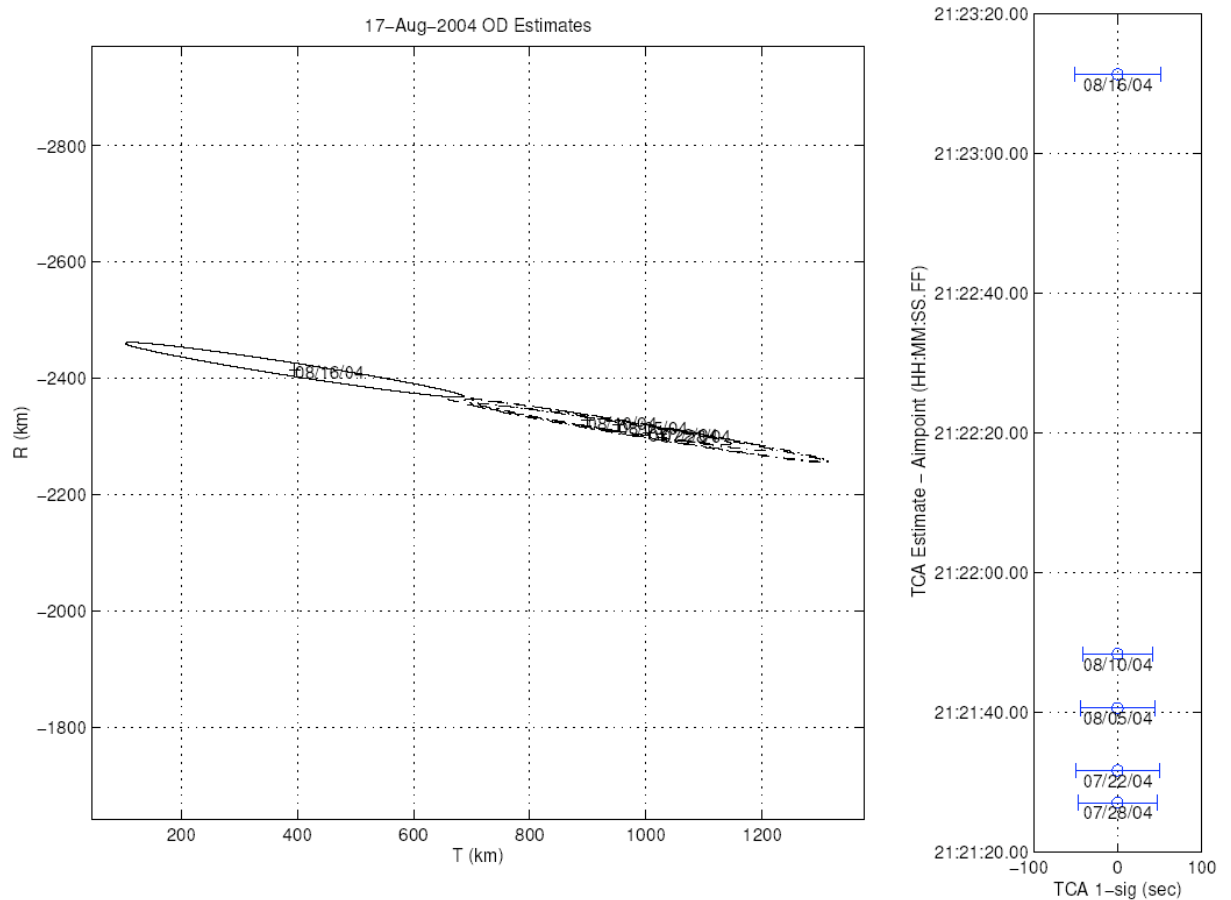
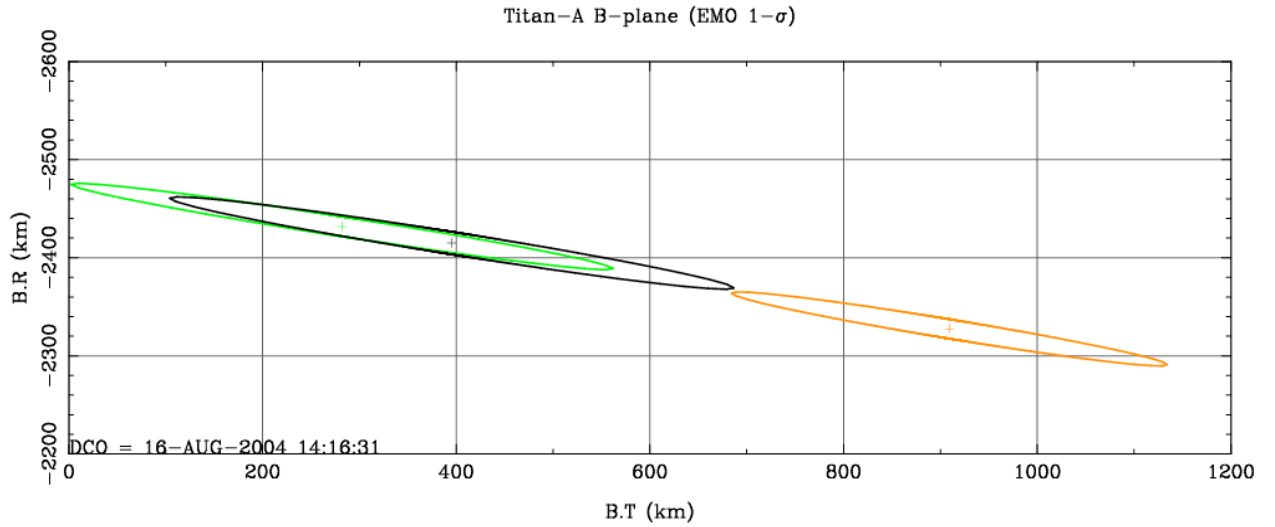
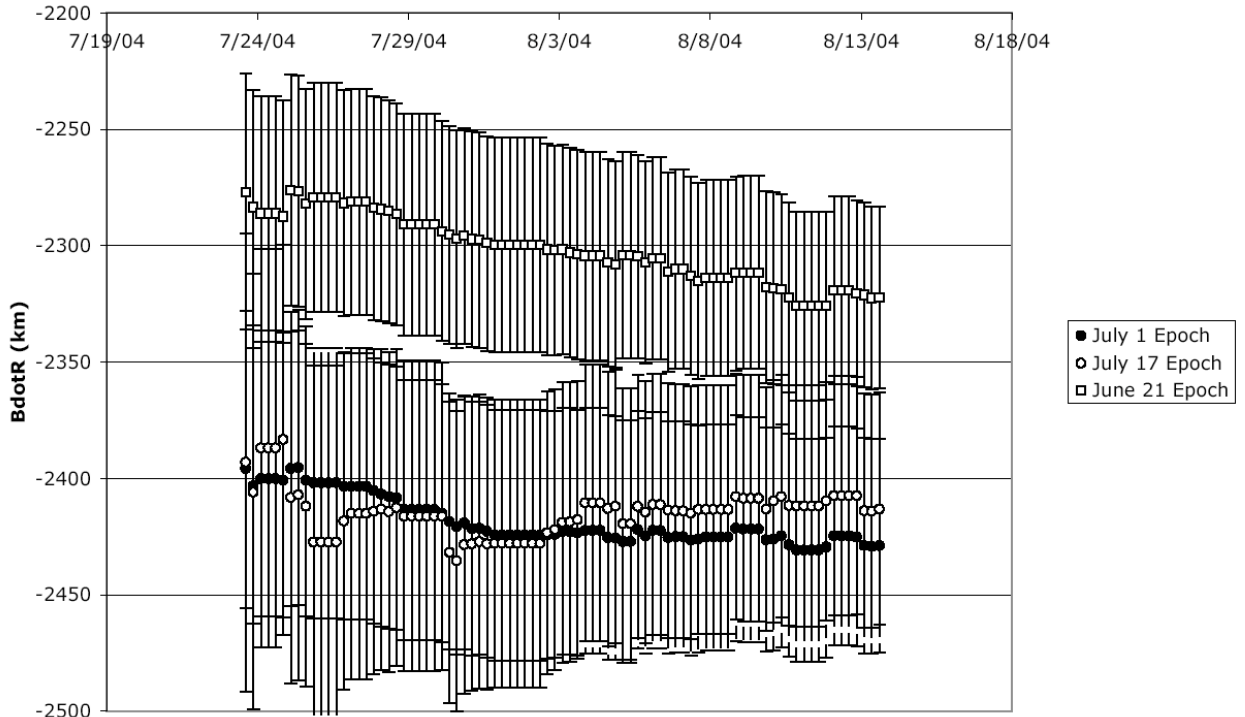


Figure 1: OTM002

This difference is shown clearly in Figure 2. This figure shows the Titan-A B-plane solutions for August 16<sup>th</sup> for three different epochs: June 21<sup>st</sup>, July 1<sup>st</sup>, and July 17<sup>th</sup>. To assist in deciding which epoch to deliver, a plot of the solution histories was computed and is shown in Figure 3. This plot shows the history of the three epochs for different data cutoffs with consistent assumptions throughout. It is readily apparent that the June 21<sup>st</sup> epoch is exhibiting a drift while the other two epochs are not.



**Figure 2: Effect of Different Epochs for OTM-002**



**Figure 3: Solution Histories for Different Epochs**

Another question to answer is the effect of various assumptions about data sets, non-gravitational forces and data weights. Excluding different types of data can test the data sets. The RTG coefficients and the stochastic accelerations constraints were varied by scales of 0.5, 2, and 10. The optical weights were also varied by comparing a range dependant weighting algorithm to a constant weight. This variety of solutions is shown below in Figure 4.

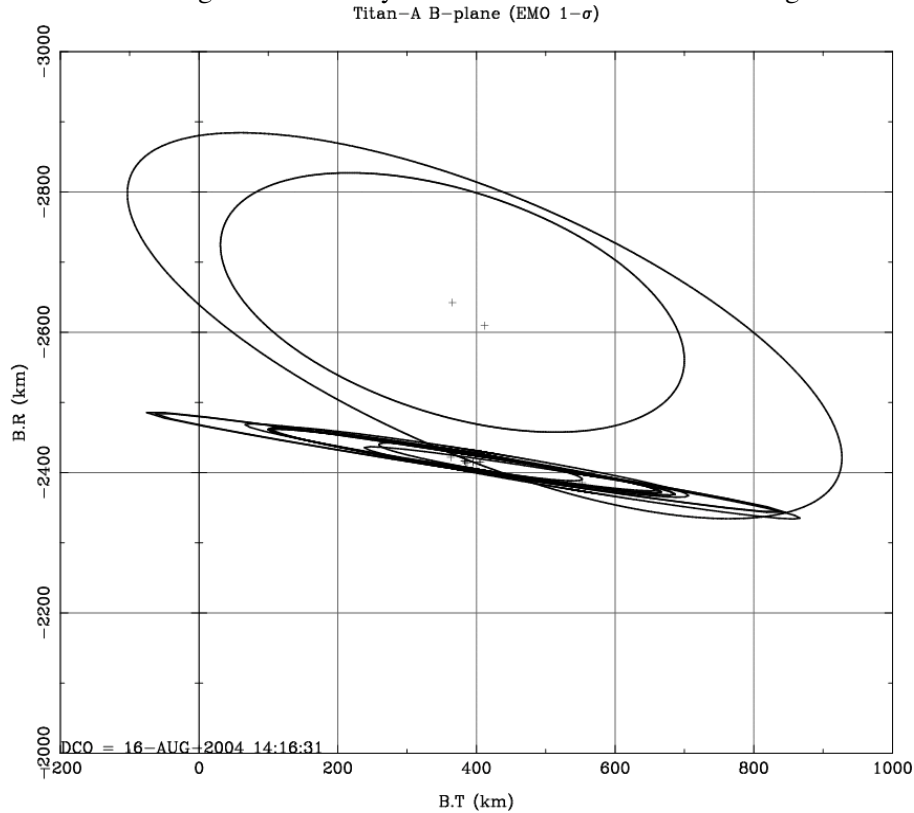


**Figure 4: Various Filter Assumptions**

The two larger ellipses are the solutions without optical data. Obviously optical data was a significant component of the solution. One can also see that the solutions agree fairly well with each other. While it is very difficult to identify one solution as the absolute best, an outlier does not exist which would signify a possible problem.

### OTM-003 Delivery

The magnitude of OTM-002 was fairly large and errors in executing such a maneuver necessitated a subsequent cleanup maneuver. This maneuver, OTM-003, was scheduled for September 7, 2004 and designed to achieve the same Titan-A B-plane target at OTM-002. The B-plane baseline solution history is shown in Figure 5. This set of ellipses shows a consistent nesting of solutions as data is added. Notice that these ellipses are of comparable size to those shown in Figure 1. The execution of a spacecraft maneuver, OTM-002, caused added a large amount of uncertainty to the predicted flyby conditions.

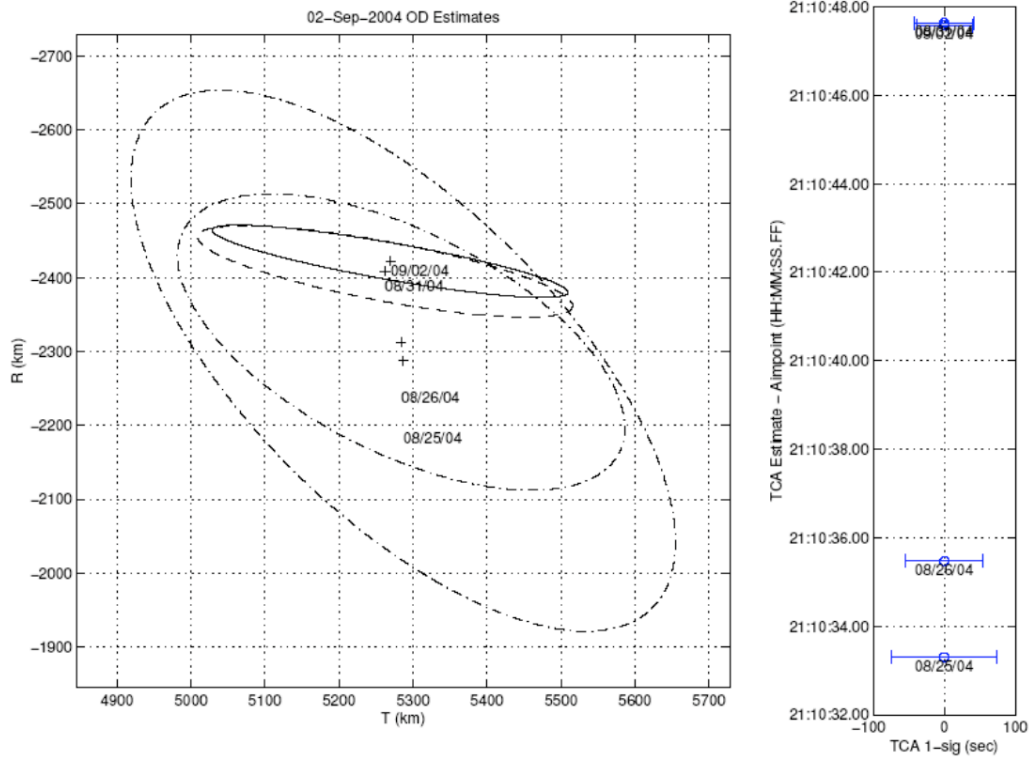


**Figure 5: History of OD Solutions for OTM-003**

A more extensive battery of alternate solutions was prepared for this maneuver as shown in Figure 6. These solutions show good agreement except for the solutions without optical data.

Another concern was the effect of opnavs of specific satellites affecting the solution. A battery of 22 solutions for a different epoch with different subsets of the satellite opnavs is shown in Figure 7. The largest ellipse contains no optical data and the second largest ellipse includes radio and Titan optical data only. One can immediately recognize that the solutions are very consistent with each other and no satellite set appears suspect. These solutions also quantify the effect of opnavs on the solutions. The Titan opnavs are improving the solution, but the other satellites are more powerful. This fact is better explained by examining the position uncertainties of Cassini and Titan with respect to the Saturn Barycenter at the predicted flyby time for three solutions (Table 4). The opnavs are helping to better determine the position of Cassini in the Saturnian system. This table also indicates that the opnavs are providing only a small improvement to the Titan ephemeris uncertainties.

**Table 4: Position Uncertainties at Flyby Time for Different Solutions**

<b>Solution</b>	<b>Cassini (km)</b>	<b>Titan (km)</b>
Radio only	103	31
Radio and Titan Optical	56	26
Radio and Optical	12	29

The Titan uncertainty increases with the additional of more optical data because of the effect of Hyperion's mass because of considering Hyperion's mass instead of estimating it. Titan is in a resonant orbit with Hyperion and even though Hyperion has a very small mass, it has an

effect on Titan. During the Saturn approach estimates of Hyperion's mass resulted in negative values and after orbit insertion the estimated value was significantly different from those expected by the science teams. Because of this behavior, the team considered Hyperion's mass instead of estimating it.

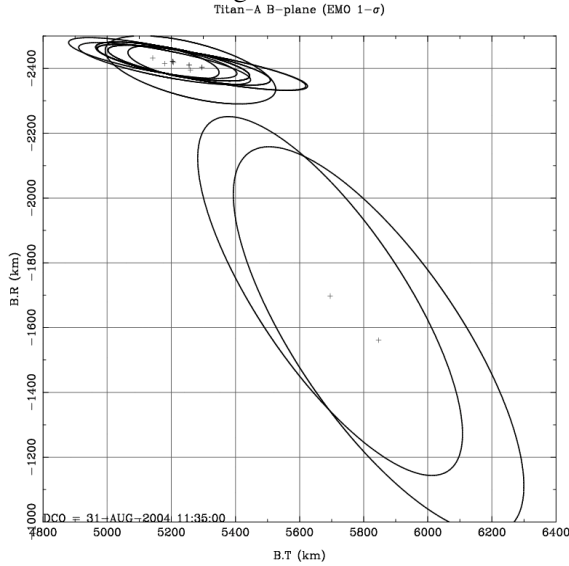


**Figure 6: Alternate Solutions**

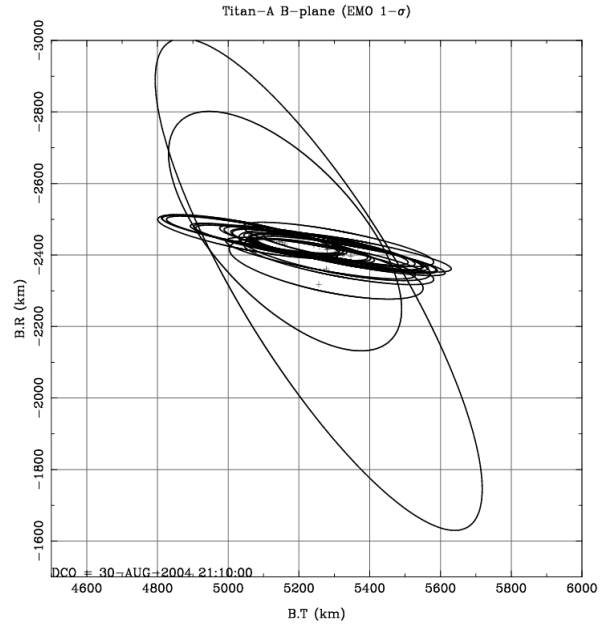


**Figure 7: Effect of Opnav Subsets**

### OTM-004 Delivery

The typical flyby sequence for Cassini includes three maneuvers. The final maneuver is designed with a zero deterministic value and is intended to remove any final errors before the flyby. The final maneuver before the Titan-A flyby was scheduled for October 23, 2004. This date placed the maneuver over 6 weeks after the previous maneuver. During this intervening time the spacecraft executed a flight software checkout and a probe release dry run. Both of these activities used a RCS control and moved the spacecraft.

The solution history prior to OTM-004 is shown in Figures 8 and 9 with the final delivery depicted with a solid ellipse.

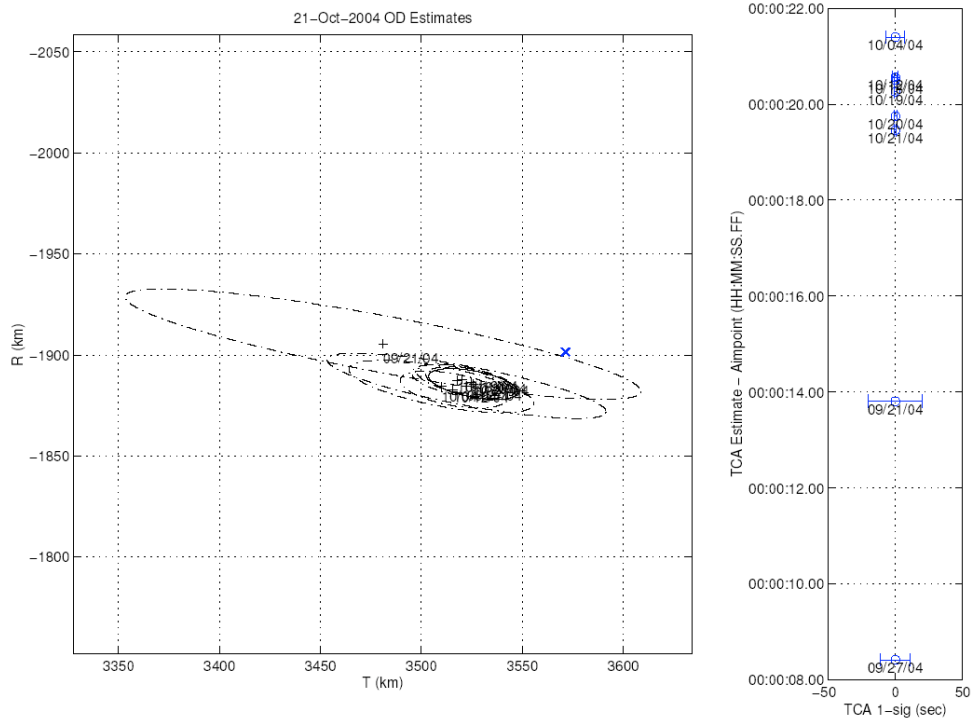


**Figure 8: History of Bplanes Solutions for OTM-004**

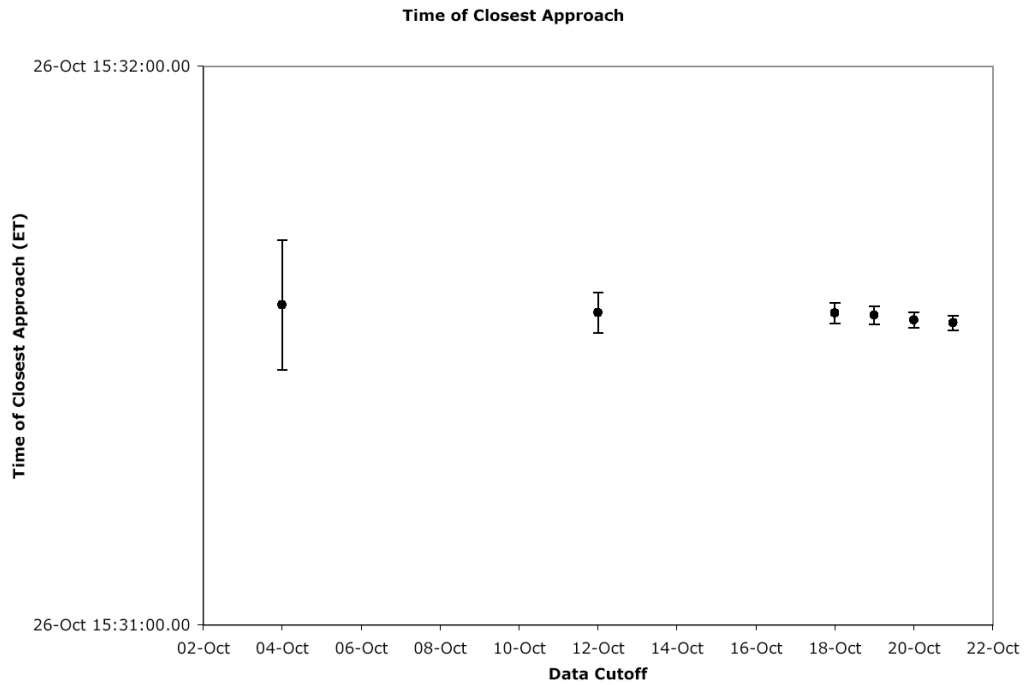


**Figure 9: History of Time of Closest Approach Solutions for OTM-004**

Another battery of solutions was computed for this final maneuver before the Titan-A flyby as shown in Figures 10-14. These figures show the effect of:

1. Different epochs,
2. Varying the constraints for the RTG acceleration, stochastic acceleration, and epoch constraints,
3. Scaling the apriori satellite covariance,
4. Varying data weights,
5. Deleting opnavs,
6. Using various data subsets.

The effect of three different epochs is shown in Figure 10. These solutions use the July 1<sup>st</sup>, July 17<sup>th</sup>, and October 5<sup>th</sup> epochs. The October 5<sup>th</sup> epoch is after a significant amount of spacecraft thrusting and excludes a significant amount of optical data but agrees very well with the other two solutions.

The constraints on the RTG coefficients, ATA values, and the epoch state were varied and these solutions are shown in Figure 11. These solutions only confirm that these parameters have relatively small effects.

The apriori satellite covariance was an important factor in the orbit determination solution. The Earth-based historical data and Cassini data prior to July 1<sup>st</sup> was processed to produce a constraint on the satellite initial conditions. A good solution would be characterized by a good agreement between the apriori constraint and the optical data after July 1<sup>st</sup>. Figure 12 shows the effect of scaling the satellite apriori covariance by 1, 3, 5, and practically infinite. These solutions agree well with each other and indicate the data before orbit insertion agrees with the data afterwards.

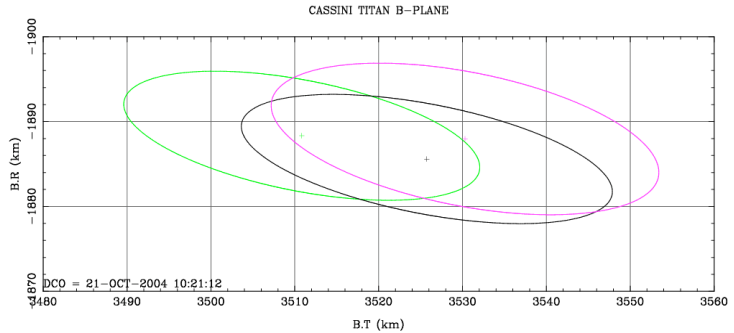


**Figure 10: Effect of Different Epochs**

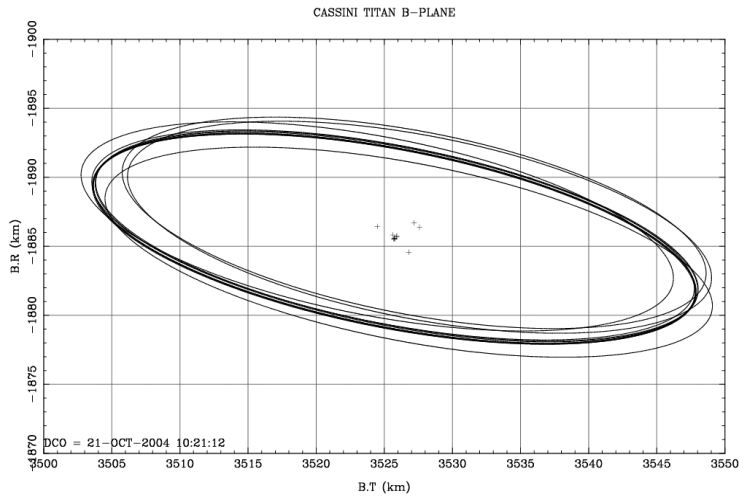


**Figure 11: Effect of Varying the RTG Acceleration,**

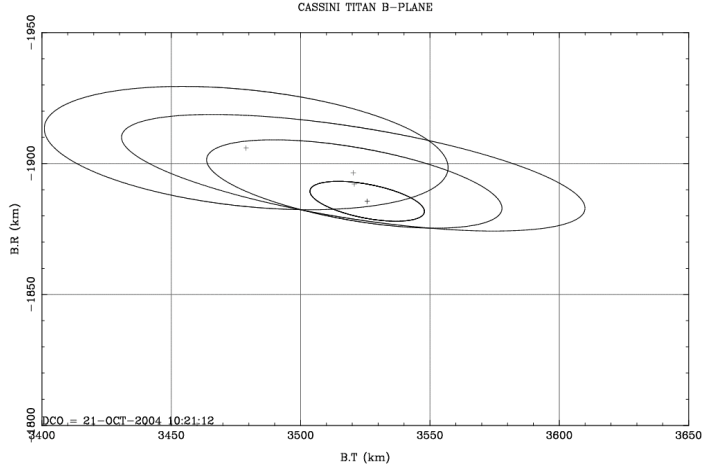


**Figure 12: Effect of Scaling Satellite Apriori Constraint**

Another concern was the effect of individual satellites on the solution. Figure 13 shows the effect of excluding one satellite's opnavs from the solution. The solutions all agree with each other; one satellite's opnavs are corrupting the solution. This figure also includes a solution with all radio and optical data except for Titan. These ellipses are Titan relative and one would assume that opnavs, or the lack thereof, would affect the solution but they do not. This topic will be revisited later.

Finally, Figure 14 shows the effect of different data subsets. The two smaller ellipses only exclude Doppler or ranging data while the two ellipses on the right both exclude optical data. The wider ellipse is an optical only solution without any radio data. This is important because such a solution has significantly different assumptions from all of the others but yields a remarkably similar solution. Based on these figures the Cassini team computed and executed OTM-004 and waited until the flyby occurred.

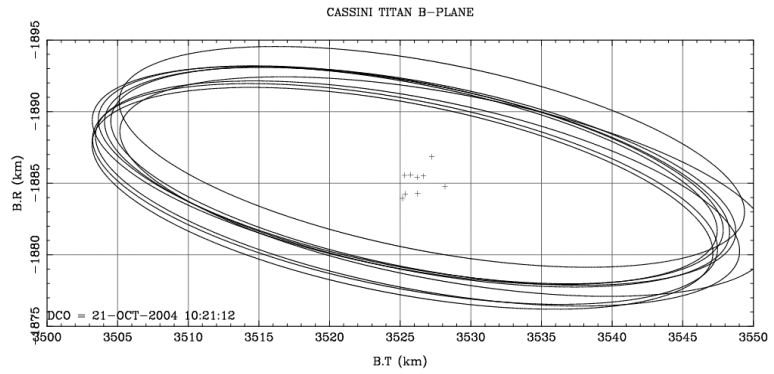


**Figure 13: Effect of Excluding Opnavs**

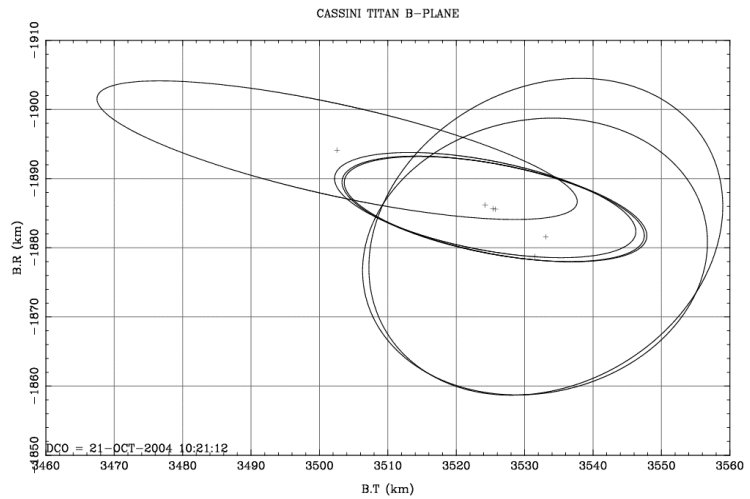


**Figure 14: Effect of Using Data Subsets**

## Post Flyby

On October 26, 2004 Cassini completed the first targeted flyby of Titan. The radiometric tracking data after the flyby was very powerful and allowed a comparison of the predicted versus reconstructed trajectory. The final pre-flyby and reconstructed solutions for the flyby are shown in Figures 15 and 16. The error ellipse and errorbars for the reconstruction are shown in the figures but are much smaller than the scale. The difference between the predicted and reconstructed are 40 km in B.T. 9 km in B.R, and 2.8 seconds in time of closest approach and 1.8, 1.2, and 4.5 sigma respectively.

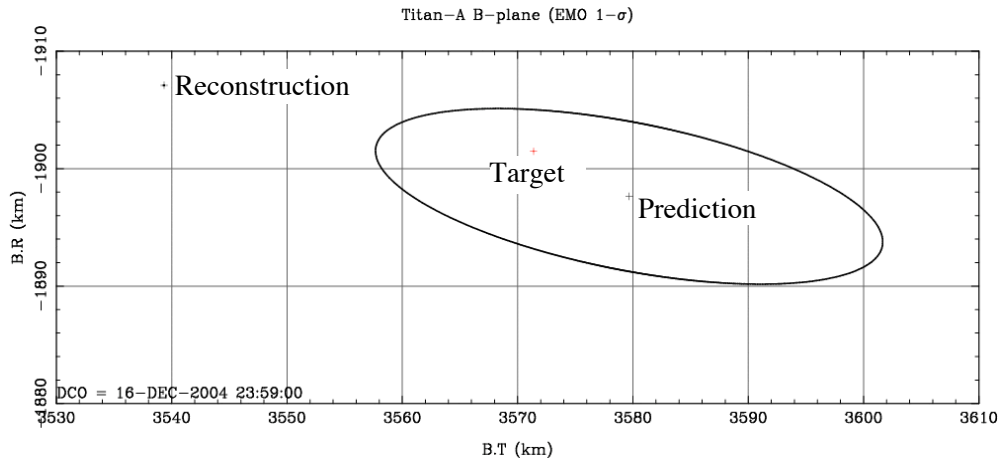


**Figure 15: Predicted and Reconstructed B-plane Values**

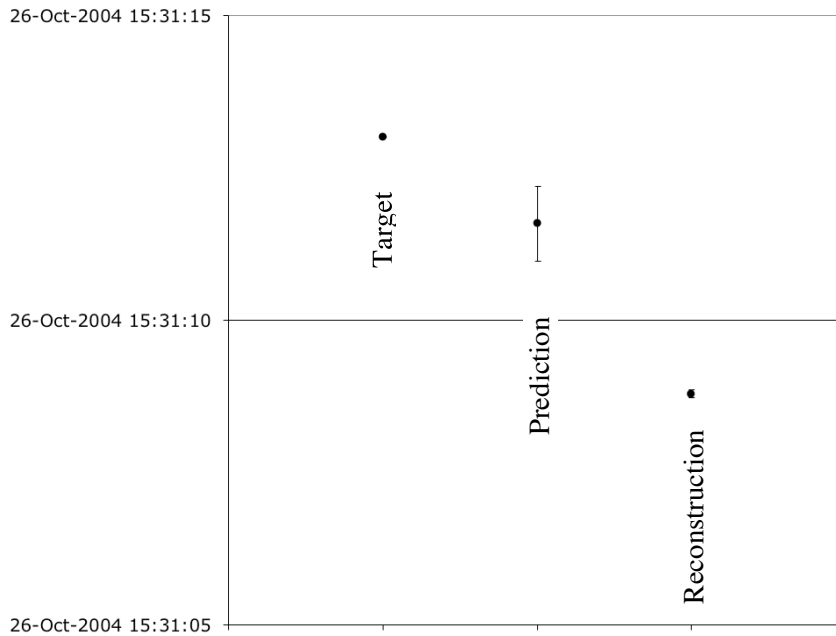


**Figure 16: Predicted and Reconstructed Time of Closest Approach Values**

The B-plane is computed from the Cassini – Titan relative trajectory. One can immediately see that Titan changed the most between these two solutions in Figure 17. This figure shows the Saturn relative position differences between the predicted and reconstructed Cassini and Titan trajectories.

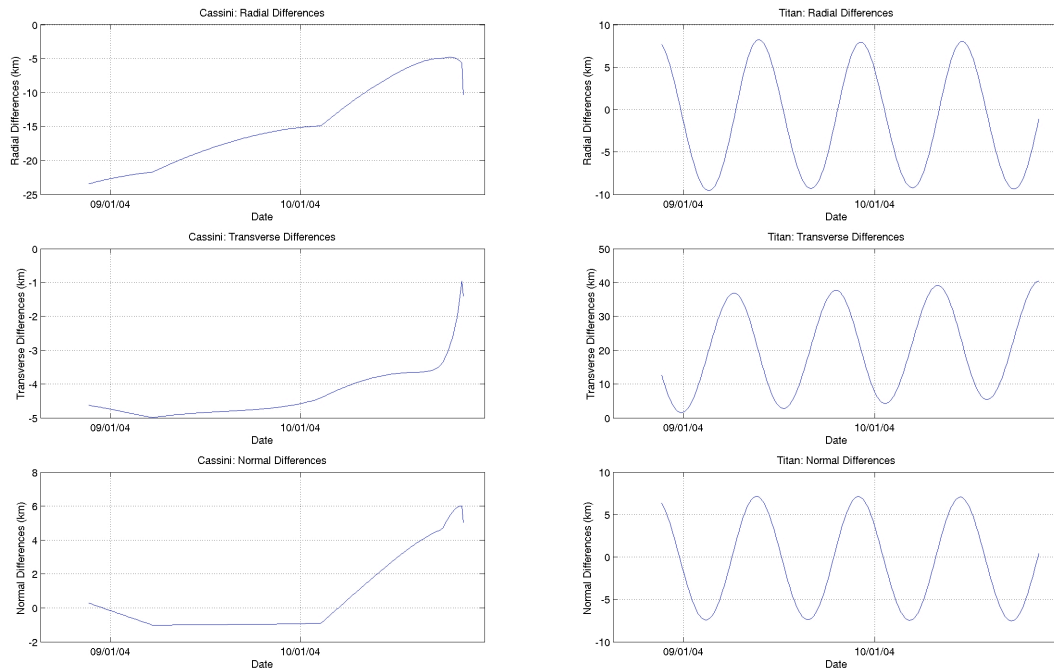


**Figure 17: Cassini and Titan Trajectories Changes Due to Post Flyby Data**

At the flyby time Cassini only shifted by 8 km but the change in Titan was 40 km although only a 20 km mean change. The shift in Titan is real because subsequent targeted flybys of Titan had considerably smaller changes in the ephemeris. The next question is why was this ephemeris difference not detected earlier?

## TITAN OBSERVABILITY

The Titan ephemeris for the orbit determination solution is driven by two factors: the apriori covariance composed of data prior to July 1<sup>st</sup> and the additional optical data. Because of the large Cassini-Titan distance and the presence of the other satellites, additional radiometric data cannot discern the Titan ephemeris outside of a flyby. The apriori covariance had a position error at the predicted flyby time of 33 by 23 by 16 km (RTN). If there were any errors in this constraint, the additional opnavs would need to reveal them.

The optical data only measures the Cassini-Titan relative position in two dimensions. The Titan ephemeris was mostly in the transverse direction but not every picture will have a good view of this direction. Another important factor is the weight used for each picture; because of Titan’s atmosphere the optical navigation team had a difficult time locating the center of Titan. To combine these two effects I computed the projection of the downtrack Titan direction into the opnav image frame and scaled by the optical weight. This value is a measure of how many kilometers of downtrack are significant in the image. These values are shown in Figure 18.

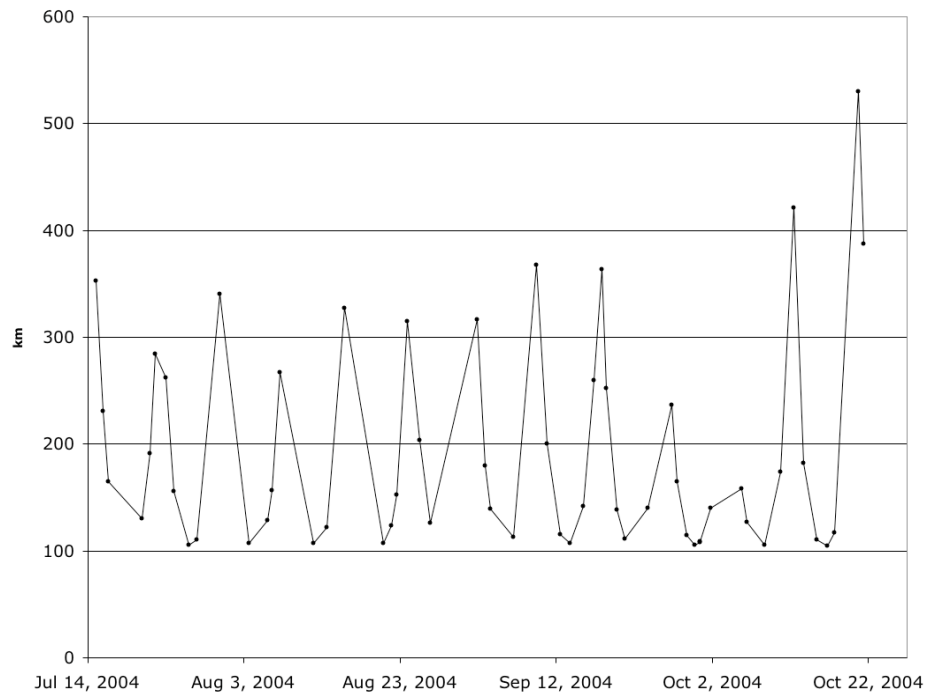


**Figure 18: Kilometers of Downtrack per Image (1-□)**

Unfortunately these values are well above the 20 km mean transverse change observed at the flyby. The optical data was not sensitive enough to discern a 20 km ephemeris change. This figure correlates well with Figure 13; the exclusion of Titan opnavs does not change the solution and indicates that no new information is being provided about the location of the target.

## CONCLUSIONS

The first targeted flyby of Titan, Titan-A, was performed by Cassini on October 26, 2004 and returned a wealth of scientific data. The orbit determination to complete this task required modeling of Cassini, Saturn, and the Saturnian satellite trajectories along with the radiometric and optical measurements. Three maneuvers were used to target this flyby and the orbit determination solutions to support each maneuver tested a wide variety of assumptions. The reconstructed flyby conditions were compared with the predicted values and revealed a shift in the Titan ephemeris. Further analysis concluded that the optical navigation images were insufficient to discern this shift.

## ACKNOWLEDGEMENTS

This research was carried out at the Jet Propulsion Laboratory, California Institute of Technology, under a contract with the National Aeronautics and Space Administration. Reference herein to any specific commercial product, process, or service by trade name, trademark, manufacturer, or otherwise, does not constitute or imply its endorsement by the United States Government or the Jet Propulsion Laboratory, California Institute of Technology.

## APPENDIX

The B-plane, shown in Figure 19, is a plane passing through the center of the target body and perpendicular to the incoming asymptote of the hyperbolic flyby trajectory. Coordinates in the plane are given in the **R** and **T** directions, with **T** being parallel to the Earth Mean Orbital plane of 2000. The angle  $\alpha$  determines the rotation of the semi-major axis of the error ellipse in the B-plane relative to the **T** axis and is measured positive right-handed about **S**.

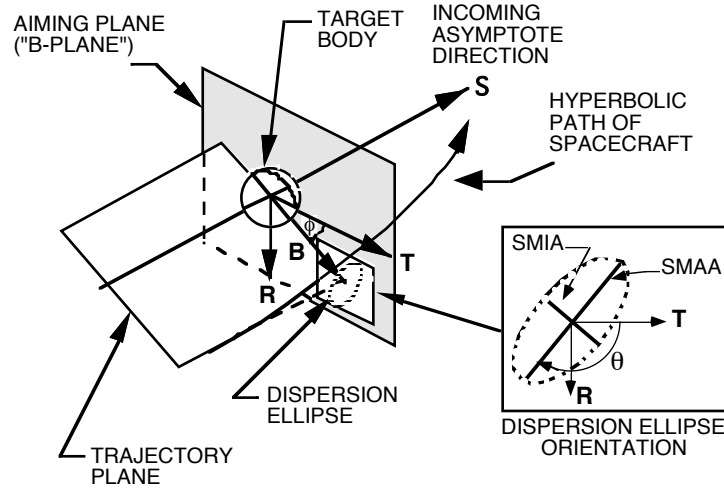


Figure 19: The B-plane Coordinate System